Environmental responses, not species interactions, determine species synchrony in natural plant communities

Andrew T. Tredennick[1*], Claire de Mazancourt[2], Michel Loreau[2], and Peter B. Adler[1]

[1]*Department of Wildland Resources and the Ecology Center, 5230 Old Main Hill, Utah State University, Logan, Utah 84322 USA*

[2]*Centre for Biodiversity Theory and Modelling, Theoretical and Experimental Ecology Station, CNRS and Paul Sabatier University, Moulis, 09200, France*

Abstract

Temporal asynchrony among species is an important mechanism through which diversity can stabilize ecosystem functioning, but identifying the mechanisms that determine synchrony remains a challenge. Here, we refine and test theory showing that synchrony depends on three factors: species responses to environmental variation, interspecific competition, and demographic stochasticity. We then conduct simulation experiments with empirical population models to quantify the relative importance of these factors in five plant communities. Simulation experiments showed that the average synchrony of per capita growth rates, which can range from 0 (perfect asynchrony) to 1 (perfect synchrony), was higher when environmental variation was present (0.62) rather than absent (0.43). Removing interspecific competition and demographic stochasticity had small effects on synchrony. In these plant communities, where species interactions and demographic stochasticity have little influence, synchrony reflects the covariance in species responses to the environment.

INTRODUCTION

Ecosystems are being transformed by species extinctions (Cardinale et al. 2012), changes in community composition (Vellend et al. 2013, Dornelas et al. 2014), and anthropogenic environmental change (Vitousek et al. 1997), impacting the provisioning and stability of ecosystem services (Loreau et al. 2001, Hooper et al. 2005, Rockstrom et al. 2009). Experiments have provided compelling evidence that decreases in species richness will decrease productivity (Tilman et al. 2001) and the temporal stability of productivity (Tilman et al. 2006, Hector et al. 2010). The stabilizing effect of species richness stems from individual

---

*Correspondence: Email: atredenn@gmail.com

species responding to environmental fluctuations (environmental stochasticity), or fluctuating asynchronously because of random chance events (demographic stochasticity) (Isbell et al. 2009, Hector et al. 2010, de Mazancourt et al. 2013). Species richness affects synchrony because larger species pools are more likely to contain species that respond disimilarly to environmental conditions (Yachi and Loreau 1999), implying that species losses will reduce ecosystem stability. Even without species losses, abiotic homogenization can weaken compensatory dynamics and, in turn, decrease temporal stability of ecosystem functioning (Hautier et al. 2014). Predicting the impacts of global change requires a mechanistic understanding of species synchrony in natural settings.

Theory identifies the three main determinants of species synchrony as environmental stochasticity, demographic stochasticity, and interspecific competition (Loreau and de Mazancourt 2008, 2013, Gonzalez and Loreau 2009). For example, in a community composed of large (no demographic stochasticity) and weakly interacting (no interspecific competition) populations, community-wide species synchrony should be determined by the covariance of species' responses to the environment (Loreau and de Mazancourt 2008). However, such a prediction relies on a relatively simple population model and only holds under two assumptions: (i) species' responses to the environment are similar in magnitude and (ii) all species have similar growth rates. Whether such theoretical predictions hold in natural communities where species differences are unlikely to be symmetrical remains unkown: no study has explicitly tested theory on the drivers of species synchrony in natural communities.

In grasslands, most empirical studies have focused on whether species synchrony is primarily an outcome of species-specific responses to environmental conditions (Hautier et al. 2014) or competition (Gross et al. 2014). Even beyond grassland studies, whether competition or environmental responses drive compensatory dynamics remains controversial (reviewed in Gonzalez and Loreau 2009). In part, controversy remains because quantifying the relative strengths of each driver on the degree of synchrony from community time series (e.g., Houlahan et al. 2007) is impossible. This is because an unbiased null expectation for synchrony does not exist (Loreau and de Mazancourt 2008) and observed synchrony can arise from non-unique combinations of factors (Ranta et al. 2008). For example, weak synchrony of population abundances could reflect positive environmental correlations (synchronizing effect) offset by strong competition (desynchronizing effect), or negative environmental correlations and weak competition.

The best way to quantify the effects of environmental stochasticity, demographic stochasticity, and interspecific competition is to remove them one-by-one, and in combination. In principle, this could be done in an extremely controlled laboratory setting, but empirically-based models of interacting populations, fit with data sets from natural communities, offer a practical alternative. For example, Mutshinda et al. (2009) fit a dynamic population model to several community time series of insect and bird abundances. They used a statistical technique to decompose temporal variation into competition and environmental components, and found that postively correlated environmental responses among species determined community dynamics. While a major step forward, Mutshinda et al.'s (2009) modeling technique relied on abundance data that may or may not reliably capture competitive interactions that occur at the individual level. Furthermore, although Mutshinda et al. (2009) quantified the relative

importance of environmental stochasticity and competition to explain the observed variation of species synchrony, they did not use the model to quantify how much synchrony would change when each factor is removed.

Here, we use multi-species population models fit to long-term demographic data from five semi-arid plant communities to test theory on the drivers of species synchrony. Our objectives are to (1) derive and test theoretical predictions of species synchrony and (2) determine the relative influence of environmental stochasticity, demographic stochasticity, and interspecific competition on species synchrony in natural plant communities. To achieve these objectives, we first refine theory that has been used to predict the effects of species richness on ecosystem stability (de Mazancourt et al. 2013) and species synchrony (Loreau and de Mazancourt 2008) to generate predictions of community-wide species synchrony under two limiting cases derived from the dynamics of individual species in monoculture. We then confront our theoretical predictions with simulations from the empirically-based population models. Second, we use the multi-species population models to perform simulation experiments that isolate the effects of environmental stochasticity, demographic stochasticity, and interspecific competition on community-wide species synchrony. Given that our population models capture the essential features of community dynamics important to synchrony (density-dependence, and demographic and environmental stochasticity), and that these models successfully reproduce observed community dynamics (Chu and Adler 2015), perturbing the models can reveal the processes that determine species synchrony in our focal grassland communities.

THEORETICAL MODEL

The model

While existing theory has identified the factors driving synchrony, we do not have a simple expression to predict synchrony in a particular community with all factors operating simultaneously. However, we can derive analytical predictions for species synchrony under special limiting cases. We focus on synchrony of per capita growth rates, rather than abundances, because growth rates represent the instantaneous response of species to the environment and competition, and are less susceptible to the legacy effects of drift and disturbance (Loreau and de Mazancourt 2008). We present equivalent results for synchrony of species abundances in the Online Supporting Information, and show that they lead to the same overall conclusions as synchrony of per capita growth rates. Following Loreau and de Mazancourt (2008) and de Mazancourt et al. (2013), we define population growth, ignoring observation error, as

$$r_i(t) = \ln N_i(t+1) - \ln N_i(t) \tag{1}$$

$$= r_{mi}\left[1 - \frac{N_i(t) + \sum_{j \neq i} \alpha_{ij} N_j(t)}{K_i} + \sigma_{ei} u_{ei}(t) + \frac{\sigma_{di} u_{di}(t)}{\sqrt{N_i(t)}}\right] \tag{2}$$

where $N_i(t)$ is the biomass of species i in year t, and $r_i(t)$ is its population growth rate in year t. r_{mi} is species i's intrinsic rate of increase, K_i is its carrying capacity, and α_{ij}

is the interspecific competition coefficient representing the effect of species j on species i. Environmental stochasticity is incorporated as $\sigma_{ei} u_{ei}(t)$, where σ_{ei}^2 is the environmental variance and u_{ei} are normal random variables with zero mean and unit variance that are independent through time but may be correlated between species. Demographic stochasticity arises from variations in births and deaths among individuals (e.g., same states, different fates), and is included in the model as a first-order, normal approximation (Lande et al. 2003, de Mazancourt et al. 2013). σ_{di}^2 is the demographic variance and $u_{di}(t)$ are independent normal variables with zero mean and unit variance. To derive analytical predictions we solved a first-order approximation of Equation 2 (de Mazancourt et al. 2013 and Online Supporting Information).

Predictions

Our first prediction assumes no interspecific interactions, no environmental stochasticity, identical intrinsic growth rates, and that demographic stochasticity is operating but all species have identical demographic variances. This limiting case, $\mathcal{M}_D$, represents a community where dynamics are driven by demographic stochasticity alone. Our prediction is

$$\phi_{R,\mathcal{M}_D} = \frac{\sum_i p_i^{-1}}{\left(\sum_i p_i^{-1/2}\right)^2} \tag{3}$$

for synchrony of per capita growth rates. p_i is the average frequency of species i, $p_i = N_i/N_T$. When all species have identical abundances and $p_i = 1/S$, where S is species richness, synchrony equal 1/S (Loreau and de Mazancourt 2008).

Our second limiting case assumes only environmental stochasticity is operating. Thus, there are no interspecific interactions, demographic stochasticity is absent, intrinsic growth rates are identical, and environmental variance is identical for all species. Our prediction for this limiting case, $\mathcal{M}_E$, is

$$\phi_{R,\mathcal{M}_E} = \frac{\sum_{i,j} \mathrm{cov}(u_{ei}, u_{ej})}{S^2} \tag{4}$$

for synchrony of per capita growth rates, where $\mathrm{cov}(u_{ei}, u_{ej})$ is the standardized covariance of environmental responses between species i and species j. Confronting our theoretical predictions with data requires estimates of species dynamics of large populations (no demographic stochasticity) in monoculture (no interspecific interactions) to calculate the covariance of species' environmental responses. To estimate environmental responses in natural communities, we turn to our population models built using long-term demographic data.

EMPIRICAL ANALYSIS

Materials and methods

Data   In the early 20th century, several range experiment stations in the western U.S. began mapping permanent quadrats, and conducted annual censuses for decades. We use such long-term demographic data sets from five semiarid grasslands in the western United States (described in detail by Chu and Adler 2015). Each study site includes a set of 1-m^2 permanent quadrats within which all individual plants were identified and mapped annually using a pantograph (Hill 1920). The resulting mapped polygons represent basal cover for grasses and canopy cover for shrubs. Data come from the Sonoran desert in Arizona (Anderson et al. 2012), sagebrush steppe in Idaho (Zachmann et al. 2010), southern mixed prairie in Kansas (Adler et al. 2007), northern mixed prairie in Montana (Anderson et al. 2011), and Chihuahuan desert in New Mexico (Anderson et al. in preparation, Chu and Adler 2015) (Table 1).

Calculating observed synchrony   The data consist of records for individual plant size in quadrats for each year. To obtain estimates of percent cover for each focal species in each year, we summed the individual-level data within quadrats and then averaged percent cover, by species, over all quadrats. We calculated per capita growth rates as $\log(x_t) - \log(x_{t-1})$, where x is species' percent cover in year t. Using the community time series of per capita growth rates or percent cover, we calculated community synchrony using the metric of Loreau and de Mazancourt (2008) in the 'synchrony' package (Gouhier and Guichard 2014) in R (R Core Team 2013). Specifically, we calculated synchrony as

$$\phi_r = \frac{\sigma_T^2}{(\sum_i \sigma_{r_i})^2} \tag{5}$$

where σ_{r_i} is the temporal variance of species i's per capita population growth rate (r_i) and σ_T^2 is the temporal variance of the aggregate community-level growth rate. ϕ ranges from 0 at perfect asynchrony to 1 at perfect synchrony (Loreau and de Mazancourt 2008). We use the same equation to calculate observed synchrony of species' percent cover, which we present to relate our results to previous findings, even though we focus on synchrony of growth rates in our model simulations (see below).

Fitting statistical models   Vital rate regressions are the building blocks of our dynamic models: an integral projection model (IPM) and an individual-based model (IBM). We followed the approach of Chu and Adler (2015) to fit statistical models for survival, growth, and recruitment (see Online Supporting Information for full details). We modeled survival probability of each genet as function of genet size, temporal variation among years, permanent spatial variation among groups of quadrats, and local neighborhood crowding from conspecific and heterospecific genets. Regression coefficients for the effect of crowding by each species can be considered a matrix of interaction coefficients whose diagonals represent intraspecific interactions and whose off-diagonals represent interspecific interactions (Adler et al. 2010). These interaction coefficients can take positive (facilitative) or negative (competitive) values. We modeled growth as the change in size of a genet from one year to the next, which depends on the same factors as the survival model. We fit the survival and growth regressions using INLA (Rue et al. 2014), a statistical package for fitting generalized linear mixed effects

models via approximate Bayesian inference (Rue et al. 2009), in R (R Core Team 2013). Genet size and crowding were treated as fixed effects; spatial (quadrat groupings) variation was treated as a random effect on the intercept and temporal (interannual) variation was treated as random effects on the intercept and the effect of genet size in the previous year (Online Supporting Information).

We modeled recruitment at the quadrat scale, rather than the individual scale, because it is impossible to attribute new genets to specific parents (Chu and Adler 2015). Our recruitment model assumes that the number of recruits produced in each year follows a negative binomial distribution with the mean dependent on the cover of the parent species, permanent spatial variation among groups, temporal variation among years, and inter- and intraspecific interactions as a function of total species' cover in the quadrat. We fit the recruitment model using a hierarchical Bayesian approach implemented in JAGS (Plummer 2003) using the 'rjags' package (Plummer 2014) in R. Again, temporal and spatial variation were treated as random effects.

Building dynamic multi-species models Once we have fit the vital rate statistical models, building the population models is straightforward. For the IBM, we initialize the model by randomly assigning plants spatial coordinates, sizes, and species identities until each species achieves a density representative of that observed in the data. We then project the model forward by using the survival regression to determine whether a genet lives or dies, the growth regression to calculate changes in genet size, and the recruitment regression to add new individuals that are distributed randomly in space. Crowding is directly calculated at each time step since each genet is spatially referenced (as in the observed data). Environmental stochasticity is not an inherent feature of IBMs, but is easily included since we fit year-specific temporal random effects for each vital rate regression. To include temporal environmental variation, at each time step we randomly choose a set of estimated survival, growth, and recruitment parameters specific to one observation year. For all simulations, we ignore the spatial random effect associated with variation among quadrat groups, so our simulations represent an average quadrat for each site.

The IPM uses the same vital rate regressions as the IBM (Rees and Ellner 2009, Rees et al. 2014), but it is spatially implicit and does not include demographic stochasticity. Following Chu and Adler (2015), we use a mean field approximation that captures the essential features of spatial patterning to define the crowding index at each time step (Supporting Online Information). Temporal variation is included in exactly the same way as for the IBM. For full details on the IPMs we use, see Chu and Adler (2015).

Simulation experiments We performed removal simulation experiments where drivers (environmental stochasticity, demographic stochasticity, or interspecific competition) were removed one-by-one and in combination. To remove interspecific interactions, we set the off-diagonals of the interaction matrix for each vital rate regression to zero. This retains intraspecific interactions, and thus density-dependence, and results in simulations where species are effectively growing in monoculture. To remove the effect of a fluctuating environment, we removed the temporal (interannual) random effects from the regression equations. To

6

remove the effect of demographic stochasticity, we use the IPM rather than the IBM because the IPM does not include demographic stochasticity (demographic stochasticity cannot be removed from the IBM). Since the effect of demographic stochasticity on population dynamics depends on population size (Lande et al. 2003), we can control the strength of demographic stochasticity by simulating the IBM on areas (e.g. plots) of different size. Indeed, results from an IBM with infinite population size would converge on results from the IPM. Given computational constraints, the largest landscape we simulate is a 25 m^2 plot.

We conducted the following six simulation experiments: (1) IBM: All drivers (environmental stochasticity, demographic stochasticity, or interspecific competition) present; (2) IPM: Demographic stochasticity removed; (3) IBM: Environmental stochasticity removed; (4) IBM: Interspecific competition removed; (5) IPM: Interspecific competition and demographic stochasticity removed; (6) IBM: Interspecific competition and environmental stochasticity removed. We ran IPM simulations for 2,000 time steps, after an initial 500 iteration burn-in period. This allowed species time to reach their stable size distribution. We then calculated the synchrony of species' per capita growth rates over 100 randomly selected contiguous 50 time-step sections. We ran IBM simulations for 100 time steps, and repeated the simulations 100 times for each simulation experiment. From those, we retained only the simulations in which no species went extinct due to demographic stochasticity. Synchrony was calculated over the 100 time steps for each no extinction run within a model experiment. To explore the effect of demographic stochasticity in different sized populations, we ran simulations (1) and (6) on plot sizes of 1, 4, 9, 16, and 25 m^2. All other IBM simulations were run on a 25 m^2 landscape.

Results from our simulation experiments also allow us to test our theoretical predictions. First, in the absence of interspecific competition and demographic stochasticity, species are effectively growing in large monocultures. Therefore, we can use results from simulation (5) to estimate the covariance of species' responses to the environment ($\text{cov}(u_{ie}, u_{je})$) and parameterize Equation 3. Parameterizing Equation 2 does not require simulation output because the only parameters are the species' relative abundances. Second, simulations (5) and (6) represent the simulated version of our limiting case theoretical predictions. Thus, we directly test the theoretical predictions by comparing them to observed synchrony and simulated synchrony.

Results

Synchrony of species' per capita growth rates at our study sites ranged from 0.36 to 0.89 and synchrony of percent cover ranged from 0.15 to 0.92 (Table 2). Synchrony tended to be higher in communities with few species (Arizona and New Mexico) and/or with relatively high temporal variability in percent cover (e.g., Montana). Synchrony was lowest in Idaho, the only data set that includes two life forms: a shrub and three perennial grasses (Table 1). For all five communities, species synchrony from IPM and IBM simulations closely approximated observed synchrony (Fig. S1). IBM-simulated synchrony is consistently, but only slightly, lower than IPM-simulated synchrony (Fig. S1), likely due to the desynchronizing effect of demographic stochasticity.

Across the five communities, our limiting case predictions closely matched synchrony from the corresponding simulation experiment (Fig. 1 and Table S1). The correlation between our analytical predictions and simulated synchrony was 0.97 for $\phi_{R,\mathcal{M}_D}$ and 0.997 for $\phi_{R,\mathcal{M}_E}$. The largest difference between predicted and simulated synchrony was 0.05 in New Mexico for $\phi_{R,\mathcal{M}_D}$ (Table S1).

Simulation experiments revealed that removing environmental fluctuations has the largest impact on synchrony, leading to a reduction in synchrony of species growth rates in four out of five communities (Fig. 1). Removing environmental fluctuations ("No E.S" simulations) decreased synchrony by 33% in Arizona, 48% in Kansas, 39% in Montana, and 40% in New Mexico. Only in Idaho did removing environmental fluctuations cause an increase in synchrony (Fig. 1), but the effect was small (9% increase; Table S2). Overall, species' temporal random effects in the statistical vital rate models are positively correlated (Table S3). Species interactions are weak in these communities (Table S4 and Chu and Adler 2015), and removing interspecific competition had little effect on synchrony (Fig. 1; "No Comp." simulations). Removing competition caused, at most, a 5% change in synchrony (Fig. 1). Removing demographic stochasticity ("No D.S." simulations) caused synchrony to increase slightly in all communities (Fig. 1), with an average 6% increase over synchrony from IBM simulations on a five meter area.

The desynchronizing effect of demographic stochasticity, which increases as population size decreases, modestly counteracted the synchronizing force of the environment, but not enough to lower synchrony to the level observed when only demographic stochasticity is operating (Fig. 2). In the largest, 25 m^2 plots, synchrony was driven by environmental stochasticity (e.g., $\mathcal{M}_E$). At 1 m^2, synchrony reflected demographic stochasticity and environmental stochasticity (e.g., between $\mathcal{M}_E$ and $\mathcal{M}_D$). For context, population sizes increased from an average of 17 individuals per community in 1 m^2 IBM simulations to an average of 357 individuals per community in 25 m^2 IBM simulations.

For all five communities, the synchrony of species' growth rates in monoculture almost perfectly matched species synchrony in polyculture (Fig. 3). Results for synchrony of percent cover are qualitatively similar, but simulation results were more variable and less consistent with analytical predictions and observed synchrony (Online Supporting Information, Figs. S2-S3).

DISCUSSION

Our study produced four main findings that were generally consistent across five natural plant communities: (1) limiting-case predictions from the theoretical model were well-supported by simulations from the empirical models; (2) demographic stochasticity decreased community synchrony, as expected by theory, and its effect was largest in small populations; (3) environmental fluctuations increased community synchrony relative to simulations in constant environments because species-specific responses to the environment were positively, though not perfectly, correlated; and (4) interspecific interactions were weak and therefore had little impact on community synchrony. We also found that analyses based on synchrony of species' percent cover, rather than growth rates, were uninformative (Figs. S2-S3) since

the linear approximation required for analytical predictions is a stronger assumption for abundance than growth rates, especially given relatively short time-series (Online Supporting Information). Thus, our results provide further evidence that it is difficult to decipher mechanisms of species synchrony from abundance time series, as expected by theory (Loreau and de Mazancourt 2008).

Simulations support theoretical predictions

Our theoretical predictions were derived from a simple model of population dynamics and required several simplifying assumptions, raising questions about their relevance to natural communities. However, the theoretical predictions were strongly supported by simulations of population models fit to long-term data from natural plant communities (Table 3). Such a close match between our analytical predictions and the simulation results should inspire confidence in the ability of simple models to inform our understanding of species synchrony. The theoretical population dynamical model we used here also successfully predicted ecosystem stability in several biodiversity-ecosystem functioning experiments (de Mazancourt et al. 2013).

Demographic stochasticity decreases synchrony

Demographic stochasticity partially counteracted the synchronizing effects of environmental fluctuations and interspecific interactions on per capita growth rates, but only when populations were small (Fig. 2), in agreement with theory (Loreau and de Mazancourt 2008). Even in small populations, however, demographic stochasticity was not strong enough to completely counteract the synchronizing effects of environmental fluctuations and match the analytical prediction where only demographic stochasticity is operating ($\mathcal{M}_D$ in Fig. 2). These results confirm the theoretical argument by Loreau and de Mazancourt (2008) that independent fluctuations among interacting species in a non-constant environment should be rare. Only in the Idaho community does synchrony of per capita growth rates approach $\mathcal{M}_D$ in a non-constant environment (Fig. 2). This is most likely due to the strong effect of demographic stochasticity on the shrub *Artemisia tripartita* since even a 5 m^2 quadrat would only contain a few individuals of that species.

Our analysis of how demographic stochasticity affects synchrony demonstrates that synchrony depends on the observation area. As the observation area increases, population size increases and the desynchronizing effect of demographic stochasticity lessens (Fig. 2). Thus, our results suggest that community-wide species synchrony will increase as the observation area increases, rising from $\mathcal{M}_D$ to $\mathcal{M}_E$. Such a conclusion assumes, however, that species richness remains constant as observation area increases, which is unlikely (Taylor 1961). Recent theoretical work has begun to explore the linkage between ecosystem stability and spatial scale (Wang and Loreau 2014, 2016), and our results suggest that including demographic stochasticity in theoretical models of metacommunity dynamics may be important for understanding the role of species synchrony in determining ecosystem stability across spatial scales.

Environmental fluctuations drive community synchrony

In large populations where interspecific interactions are weak, synchrony is expected to be driven exclusively by environmental fluctuations (Equation 4). Under such conditions community synchrony should approximately equal the synchrony of species' responses to the environment (Loreau and de Mazancourt 2008). Two lines of evidence lead us to conclude that environmental fluctuations drive species synchrony in our focal plant communities. First, in our simulation experiments, removing interspecific interactions resulted in no discernible change in community-wide species synchrony of per capita growth rates (Fig. 1). Second, removing environmental fluctuations from simulations consistently reduced synchrony (Fig. 1), and the synchrony of species in monoculture was a very strong predictor of synchrony of species in polyculture (Fig. 3). Our results lead us to conclude that environmental fluctuations, not species interactions, are the primary driver of community-wide species synchrony in the communities we studied. Given accumulating evidence that niche differences in natural communities are large (reviewed in Chu and Adler 2015), and thus species interactions are likely to be weak, our results may be general in natural plant communities.

In the Idaho community, removing environmental fluctuations did not cause a large decrease in synchrony. However, that result appears to be an artifact. Removing environmental variation results in a negative invasion growth rate for *A. tripartita*. Although we only analyzed IBM runs in which *A. tripartita* had not yet gone extinct, it was at much lower abundance than in the other simulation runs. When we removed *A. tripartita* from all simulations, the Idaho results conformed with results from all other sites: removing environmental stochasticity caused a significant reduction in species synchrony (Fig. S4). Our main results for Idaho (Fig. 2), with *A. tripartita* included, demonstrate how the processes that determine species synchrony interact in complex ways. *A. tripartita* has a facilitative effect on each grass species across all vital rates, except for a small competitive effect on *H. comata*'s survival probability (Tables S8-S10). At the same time, all the perennial grasses have negative effects on each other for each vital rate (Tables S8-S10). We know synchrony is affected by interspecific competition (Loreau and de Mazancourt 2008), but how facilitative effects manifest themselves is unknown. The interaction of facilitation and competition is clearly capable of having a large effect on species synchrony, and future theoretical efforts should aim to include a wider range of species interactions.

A challenge to the generality of our results is that we were only able to model common, co-occuring species (see Chu and Adler 2015). Rare species, which our analysis does not include, could be kept at low densities by competitive suppression due to strong interspecific interactions. If we had been able to model rare species, we might have found a larger effect of competition on community synchrony. However, rare species may occupy rare niches that do not overlap with other species, in which case synchrony would remain predominantly driven by environmental responses. Rare species could also be limited by generalist natural enemies whose effects are density-independent but alter competitive hierarchies (Mordecai 2011). Under such conditions, synchrony will depend on the degree of pathogen-induced fitness differences and the pathogen's response to environmental conditions. Neither our model nor current theory explicitly considers the effects of pathogens on species synchrony, and this highlights the need for theoretical work on the interaction between mechanisms of

species coexistence and mechanisms of species synchrony (Loreau 2010).

Interspecific interactions had little impact on community synchrony

We expected community synchrony of per capita growth rates to decrease when we removed interspecific interactions (Loreau and de Mazancourt 2008). We found that community synchrony was virtually indistinguishable between simulations with and without interspecific interactions (Fig. 2). The lack of an effect of interspecific competition on synchrony is in contrast to a large body of theoretical work that predicts a strong role for competition in creating compensatory dynamics (Tilman 1988) and a recent empirical analysis (Gross et al. 2014).

Our results do not contradict the idea that competition can lead to compensatory dynamics, but they do highlight the fact that interspecific competition must be relatively strong to influence species synchrony. The communities we analyzed are composed of species with very little niche overlap (Chu and Adler 2015) and weak interspecific interactions (Tables S1, S3-S17). Mechanistic consumer-resource models (Lehman and Tilman 2000) and phenomenological Lotka-Volterra models (Lehman and Tilman 2000, Loreau and de Mazancourt 2013) both confirm that the effect of competition on species synchrony diminishes as niche overlap decreases. In that sense, our results are not surprising: interspecific interactions are weak, so of course removing them does not affect synchrony.

However, our results do contrast with a recent analysis of several biodiversity-ecosystem functioning experiments showing that competition drives species synchrony in grasslands (Gross et al. 2014). The apparent inconsistency between our results and those of Gross et al. (2014) may be explained by the differences between our studies. Gross et al.'s results are based on rapidly assembling experimental communities that are, at most, 11 years old. The natural, relatively undisturbed communities we studied consist of species that have co-occurred for decades (Chu and Adler 2015) and represent a much later stage of community assembly. In theory, species interactions should weaken through time as community assembly proceeds (Kokkoris et al. 1999), meaning that in biodiversity-ecosystem functioning experiments the processes driving competitive exclusion are still operating. Such communities may be highly influenced by transient, but strong, interspecific competition that can mask the synchronizing effects of the environment. In contrast, synchrony may be driven by environmental fluctuations in older communities. In other words, the dominant driver of community synchrony should shift from competition to environmental fluctuations through time. One way to test this prediction is to continue collecting data from biodiversity-ecosystem functioning experiments and conduct the analysis of Gross et al. (2014) every few years.

CONCLUSIONS

Species-specific responses to temporally fluctuating environmental conditions is an important mechanism underlying asynchronous population dynamics and, in turn, ecosystem stability (Loreau and de Mazancourt 2013). When we removed environmental variation, we found that synchrony decreased in four out of the five grassland communities we studied (Fig. 2).

A tempting conclusion is that our study confirms that compensatory dynamics are rare in natural communities, and that ecologically-similar species will exhibit synchronous dynamics (e.g., Houlahan et al. 2007). Such a conclusion misses an important subtlety. The perennial grasses we studied do have similar responses to the environment (Table S2), which will tend to synchronize dynamics. However, if community-wide species synchrony is less than 1, as it is in all our focal communities, some degree of compensatory dynamics must be present (Loreau and de Mazancourt 2008). In agreement with other studies (Rocha et al. 2011, Vasseur et al. 2014), we find that environmental responses are primarily responsible for the degree of synchrony among ecologically-similar species. This result contrasts with a recent analysis of several biodiversity-ecosystem functioning experiments showing that competition drives community synchrony (Gross et al. 2014). Recently assembled communities, such as experimental plots, may exhibit strong species interactions that will weaken over time (Kokkoris et al. 1999). Future research on the influence of community assembly on synchrony could reconcile inconsistent observations on the biotic and abiotic forces that jointly drive community dynamics.

ACKNOWLEDGMENTS

STATEMENT OF AUTHORSHIP

ATT, CdM, and PBA designed the research. CdM and ML designed and analyzed the theoretical model. ATT and PBA performed the empirical analysis. All authors contributed to the interpretation and presentation of results. ATT wrote the first draft of the manuscript, and all authors contributed to manuscript revisions.

References

Adler, P. B., S. P. Ellner, and J. M. Levine. 2010. Coexistence of perennial plants: An embarrassment of niches. Ecology Letters 13:1019–1029.

Adler, P. B., W. R. Tyburczy, and W. K. Lauenroth. 2007. Long-term mapped quadrats from Kansas prairie: demographic information for herbaceous plants. Ecology 88:2673.

Anderson, J., M. P. McClaran, and P. B. Adler. 2012. Cover and density of semi-desert grassland plants in permanent quadrats mapped from 1915 to 1947. Ecology 93:1492–1492.

Anderson, J., L. Vermeire, and P. B. Adler. 2011. Fourteen years of mapped, permanent quadrats in a northern mixed prairie, USA. Ecology 92:1703.

Cardinale, B. J., J. E. Duffy, A. Gonzalez, D. U. Hooper, C. Perrings, P. Venail, A. Narwani, G. M. Mace, D. Tilman, D. A. Wardle, A. P. Kinzig, G. C. Daily, M. Loreau, and J. B. Grace. 2012. Biodiversity loss and its impact on humanity. Nature 489:59–67.

Chu, C., and P. B. Adler. 2015. Large niche differences emerge at the recruitment stage to stabilize grassland coexistence. Ecological Monographs 85:373–392.

de Mazancourt, C., F. Isbell, A. Larocque, F. Berendse, E. De Luca, J. B. Grace, B. Haegeman, H. Wayne Polley, C. Roscher, B. Schmid, D. Tilman, J. van Ruijven, A. Weigelt, B. J. Wilsey, and M. Loreau. 2013. Predicting ecosystem stability from community composition and biodiversity. Ecology Letters 16:617–625.

Dornelas, M., N. J. Gotelli, B. McGill, H. Shimadzu, F. Moyes, C. Sievers, and A. E. Magurran. 2014. Assemblage time series reveal biodiversity change but not systematic loss. Science 344:296–9.

Gonzalez, A., and M. Loreau. 2009. The Causes and Consequences of Compensatory Dynamics in Ecological Communities. Annual Review of Ecology, Evolution, and Systematics 40:393–414.

Gouhier, T. C., and F. Guichard. 2014. Synchrony: quantifying variability in space and time. Methods in Ecology and Evolution 5:524–533.

Gross, K., B. J. Cardinale, J. W. Fox, A. Gonzalez, M. Loreau, H. W. Polley, P. B. Reich, and J. van Ruijven. 2014. Species richness and the temporal stability of biomass production: a new analysis of recent biodiversity experiments. The American naturalist 183:1–12.

Hautier, Y., E. W. Seabloom, E. T. Borer, P. B. Adler, W. S. Harpole, H. Hillebrand, E. M. Lind, A. S. MacDougall, C. J. Stevens, J. D. Bakker, Y. M. Buckley, C. Chu, S. L. Collins, P. Daleo, E. I. Damschen, K. F. Davies, P. a Fay, J. Firn, D. S. Gruner, V. L. Jin, J. a Klein, J. M. H. Knops, K. J. La Pierre, W. Li, R. L. McCulley, B. a Melbourne, J. L. Moore, L. R. O'Halloran, S. M. Prober, A. C. Risch, M. Sankaran, M. Schuetz, and A. Hector. 2014. Eutrophication weakens stabilizing effects of diversity in natural grasslands. Nature 508:521–5.

Hector, A., Y. Hautier, P. Saner, L.Wacker, R. Bagchi, J. Joshi, M. Scherer-Lorenzen, E. M. Spehn, E. Bazeley-White, M.Weilenmann, M. C. Caldeira, P. G. Dimitrakopoulos, J. a. Finn, K. Huss-Danell, A. Jumpponen, and M. Loreau. 2010. General stabilizing effects of plant

diversity on grassland productivity through population asynchrony and overyielding. Ecology 91:2213–2220.

Hooper, D., F. Chapin III, and J. Ewel. 2005. Effects of biodiversity on ecosystem functioning: a consensus of current knowledge. Ecological Monographs 75:3–35.

Houlahan, J. E., D. J. Currie, K. Cottenie, G. S. Cumming, S. K. M. Ernest, C. S. Findlay, S. D. Fuhlendorf, U. Gaedke, P. Legendre, J. J. Magnuson, B. H. McArdle, E. H. Muldavin, D. Noble, R. Russell, R. D. Stevens, T. J. Willis, I. P. Woiwod, and S. M. Wondzell. 2007. Compensatory dynamics are rare in natural ecological communities. Proceedings of the National Academy of Sciences of the United States of America 104:3273–3277.

Isbell, F. I., H. W. Polley, and B. J. Wilsey. 2009. Biodiversity, productivity and the temporal stability of productivity: Patterns and processes. Ecology Letters 12:443–451.

Kokkoris, G. D., A. Y. Troumbis, and J. H. Lawton. 1999. Patterns of species interaction strength in assembled theoretical competition communities. Ecology Letters 2:70–74.

Lande, R., S. Engen, and B.-E. Saether. 2003. Stochastic population dynamics in ecology and conservation.

Lehman, C. L., and D. Tilman. 2000. Biodiversity, Stability, and Productivity in Competitive Communities. The American Naturalist 156:534–552.

Loreau, M. 2010. From Populations to Ecosystems: Theoretical Fondations for a New Ecological Synthesis.

Loreau, M., and C. de Mazancourt. 2008. Species synchrony and its drivers: neutral and nonneutral community dynamics in fluctuating environments. The American Naturalist 172:E48–E66.

Loreau, M., and C. de Mazancourt. 2013. Biodiversity and ecosystem stability: A synthesis of underlying mechanisms. Ecology Letters 16:106–115.

Loreau, M., S. Naeem, P. Inchausti, J. Bengtsson, J. P. Grime, A. Hector, D. U. Hooper, M. A. Huston, D. Raffaelli, B. Schmid, D. Tilman, and D. A. Wardle. 2001. Biodiversity and ecosystem functioning: current knowledge and future challenges. Science 294:804–808.

Mordecai, E. A. 2011. Pathogen impacts on plant communities: Unifying theory, concepts, and empirical work. Ecological Monographs 81:429–441.

Mutshinda, C. M., R. B. O'Hara, and I. P. Woiwod. 2009. What drives community dynamics? Proceedings of the Royal Society B: Biological Sciences 276:2923–2929.

Plummer, M. 2003. JAGS: A Program for Analysis of Bayesian Graphical Models Using Gibbs Sampling. Pages 20–22 *in* Proceedings of the 3rd international workshop on distributed statistical computing (dSC 2003). march.

Plummer, M. 2014. rjags: Bayesian graphical models using MCMC.

R Core Team. 2013. R: A language and environment for statistical computing.

Ranta, E., V. Kaitala, M. S. Fowler, J. Laakso, L. Ruokolainen, and R. O'Hara. 2008. Detecting compensatory dynamics in competitive communities under environmental forcing. Oikos 117:1907–1911.

Rees, M., and S. P. Ellner. 2009. Integral projection models for populations in temporally varying environments. Ecological Monographs 79:575–594.

Rees, M., D. Z. Childs, and S. P. Ellner. 2014. Building integral projection models: A user's guide.

Rocha, M. R., U. Gaedke, and D. a. Vasseur. 2011. Functionally similar species have similar dynamics. Journal of Ecology 99:1453–1459.

Rockstrom, J., J. Rockstrom, W. Steffen, W. Steffen, K. Noone, K. Noone, A. Persson, A. Persson, F. S. Chapin, F. S. Chapin, E. F. Lambin, E. F. Lambin, T. M. Lenton, T. M. Lenton, M. Scheffer, M. Scheffer, C. Folke, C. Folke, H. J. Schellnhuber, H. J. Schellnhuber, B. Nykvist, B. Nykvist, C. A. de Wit, C. A. de Wit, T. Hughes, T. Hughes, S. van der Leeuw, S. van der Leeuw, H. Rodhe, H. Rodhe, S. Sorlin, S. Sorlin, P. K. Snyder, P. K. Snyder, R. Costanza, R. Costanza, U. Svedin, U. Svedin, M. Falkenmark, M. Falkenmark, L. Karlberg, L. Karlberg, R. W. Corell, R. W. Corell, V. J. Fabry, V. J. Fabry, J. Hansen, J. Hansen, B. Walker, B. Walker, D. Liverman, D. Liverman, K. Richardson, K. Richardson, P. Crutzen, P. Crutzen, J. A. Foley, and J. A. Foley. 2009. A safe operating space for humanity. Nature 461:472–475.

Rue, H., S. Martino, and N. Chopin. 2009. Approximate Bayesian Inference for Latent Gaussian Models Using Integrated Nested Laplace Approximations. Journal of the Royal Statistical Society, Series B 71:319–392.

Rue, H., S. Martino, F. Lindgren, D. Simpson, A. Riebler, and E. Teixeira. 2014. INLA: Functions which allow to perform full Bayesian analysis of latent Gaussian models using Integrated Nested Laplace Approximaxion.

Taylor, L. R. 1961. Aggregation, Variance and the Mean. Nature 189:732–735.

Tilman, D. 1988. Plant strategies and the dynamics and structure of plant communities. Plant strategies and the dynamics and structure of plant communities.:360 pp.

Tilman, D., P. B. Reich, and J. M. H. Knops. 2006. Biodiversity and ecosystem stability in a decade-long grassland experiment. Nature 441:629–632.

Tilman, D., P. B. Reich, J. Knops, D. Wedin, T. Mielke, and C. Lehman. 2001. Diversity and productivity in a long-term grassland experiment. Science 294:843–845.

Vasseur, D. a, J. W. Fox, A. Gonzalez, R. Adrian, B. E. Beisner, M. R. Helmus, C. Johnson, P. Kratina, C. Kremer, C. de Mazancourt, E. Miller, W. a Nelson, M. Paterson, J. a Rusak, J. B. Shurin, and C. F. Steiner. 2014. Synchronous dynamics of zooplankton competitors prevail in temperate lake ecosystems. Proceedings. Biological sciences / The Royal Society 281:20140633.

Vellend, M., L. Baeten, I. H. Myers-Smith, S. C. Elmendorf, R. Beauséjour, C. D. Brown, P. De Frenne, K. Verheyen, and S. Wipf. 2013. Global meta-analysis reveals no net change in local-scale plant biodiversity over time. Proceedings of the National Academy of Sciences of the United States of America 110:19456–9.

Vitousek, P. M., H. a Mooney, J. Lubchenco, and J. M. Melillo. 1997. Human Domination of Earth' s Ecosystems. Science 277:494–499.

Wang, S., and M. Loreau. 2014. Ecosystem stability in space: α, β and γ variability. Ecology Letters 17:891–901.

Wang, S., and M. Loreau. 2016. Biodiversity and ecosystem stability across scales in metacommunities. Ecology Letters.

Yachi, S., and M. Loreau. 1999. Biodiversity and ecosystem productivity in a fluctuating environment: the insurance hypothesis. Proceedings of the National Academy of Sciences of the United States of America 96:1463–1468.

Zachmann, L., C. Moffet, and P. Adler. 2010. Mapped quadrats in sagebrush steppe: long-term data for analyzing demographic rates and plant–plant interactions. Ecology 91:3427.

Table Titles

TABLE 1: Site descriptions and focal species.

TABLE 2: Observed synchrony among species' per capita growth rates (ϕ_R), observed synchrony among species' percent cover (ϕ_C), the coefficient of variation of total community cover, and species richness for each community. Species richness values reflect the number of species analyzed from the community, not the actual richness.

Tables

Table 1: Site descriptions and focal species.

Site Name	Biome	Location (Lat, Lon)	Obs. Years	Species
New Mexico	Chihuahuan Desert	32.62° N, 106.67° W	1915-1950	*Bouteloua eriopoda*
				Sporobolus flexuosus
Arizona	Sonoran Desert	31°50' N, 110°53' W	1915-1933	*Bouteloua eriopoda*
				Bouteloua rothrockii
Kansas	Southern mixed prairie	38.8° N, 99.3° W	1932-1972	*Bouteloua curtipendula*
				Bouteloua hirsuta
				Schizachyrium scoparium
Montana	Northern mixed prairie	46°19' N, 105°48' W	1926-1957	*Bouteloua gracilis*
				Hesperostipa comata
				Pascopyrum smithii
				Poa secunda
Idaho	Sagebrush steppe	44.2° N, 112.1° W	1926-1957	*Artemisia tripartita*
				Pseudoroegneria spicata
				Hesperostipa comata
				Poa secunda

Table 2: Observed synchrony among species' per capita growth rates (ϕ_R), observed synchrony among species' percent cover (ϕ_C), the coefficient of variation of total community cover, and species richness for each community. Species richness values reflect the number of species analyzed from the community, not the actual richness.

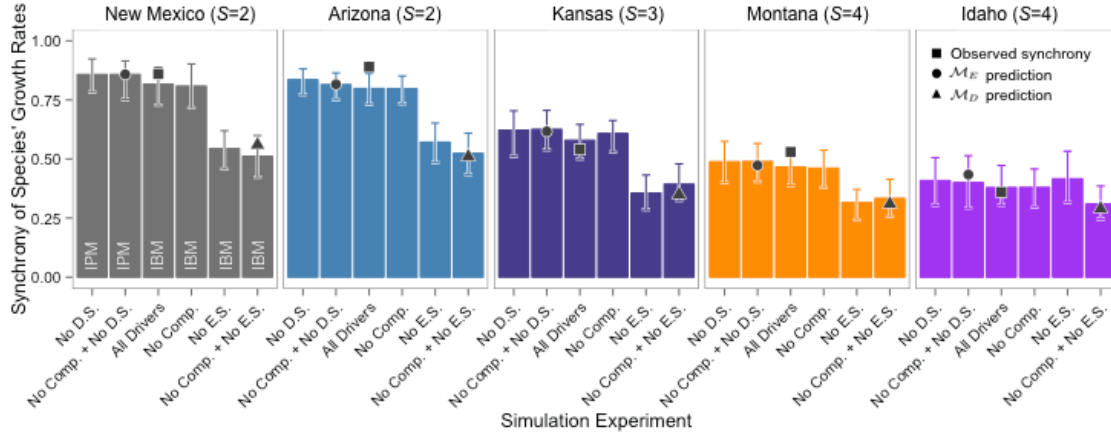| Site	ϕ_R	ϕ_C	CV of Total Cover	Species richness
New Mexico	0.86	0.92	0.51	2
Arizona	0.89	0.80	0.47	2
Kansas	0.54	0.15	0.30	3
Montana	0.53	0.58	0.54	4
Idaho	0.36	0.18	0.19	4

Figures Captions

FIGURE 1: Community-wide species synchrony of per capita growth rates from model simulation experiments. Synchrony of species' growth rates for each study area are from simulation experiments with demographic stochasticity, environmental stochasticity, and interspecific competition present ("All Drivers"), demographic stochasticity removed ("No D.S."), environmental stochasticity removed ("No E.S."), interspecific competition removed ("No Comp."), interspecific competition and demographic stochasticity removed ("No Comp. + No D.S."), and interspecific competition and environmental stochasticity removed ("No Comp. + No E.S."). Abbreviations within the bars for the New Mexico site indicate whether the IBM or IPM was used for a particular simulation. Error bars represent the upper and lower 95% quantiles from model simulations. All IBM simulations shown in this figure were run on a 25 m^2 virtual landscape. Points show observed and predicted synchrony aligned with the model simulation that corresponds with each observation or analytical prediction.

FIGURE 2: Synchrony of species' growth rates for each study area from IBM simulations across different landscape sizes when only demographic stochastcity is present ("D.S. Only") and when environmental stochasticity is also present removed ("D.S. + E.S."). The horizontal lines show the analytical predictions $\mathcal{M}_D$ (dashed line) and $\mathcal{M}_E$ (dotted line). The strength of demographic stochasticity decreases as landscape size increases because population sizes also increase. Theoretically, "D.S. Only" simulations should remain constant across landscape size, whereas "D.S. + E.S." simulations should shift from the $\mathcal{M}_D$ prediction to the $\mathcal{M}_E$ prediction as landscape size, and thus population size, increases, but only if demographic stochasticity it strong enough to counteract environmental forcing. Error bars represent the upper and lower 95% quantiles from model simulations.

FIGURE 3: Synchrony of species per capita growth rates simulated in large monocultures (IPM without species interactions) versus synchrony in large polycultures (IPM with species interactions). We used the same sequence of random year effects for both simulations

(monoculture and polyculture) to mimic biodiversity-ecosystem functioning experiments. The dashed line is the line of equality. Simulation results in this figure are analogous to "No Comp. + No D.S." (monocultures) and "No D.S." (polycultures) in Fig. 1, but here we control the time series of random year effects.

Figures

Figure 1: Community-wide species synchrony of per capita growth rates from model simulation experiments. Synchrony of species' growth rates for each study area are from simulation experiments with demographic stochasticity, environmental stochasticity, and interspecific competition present ("All Drivers"), demographic stochasticity removed ("No D.S."), environmental stochasticity removed ("No E.S."), interspecific competition removed ("No Comp."), interspecific competition and demographic stochasticity removed ("No Comp. + No D.S."), and interspecific competition and environmental stochasticity removed ("No Comp. + No E.S."). Abbreviations within the bars for the New Mexico site indicate whether the IBM or IPM was used for a particular simulation. Error bars represent the upper and lower 95% quantiles from model simulations. All IBM simulations shown in this figure were run on a 25 m^2 virtual landscape. Points show observed and predicted synchrony aligned with the model simulation that corresponds with each observation or analytical prediction.
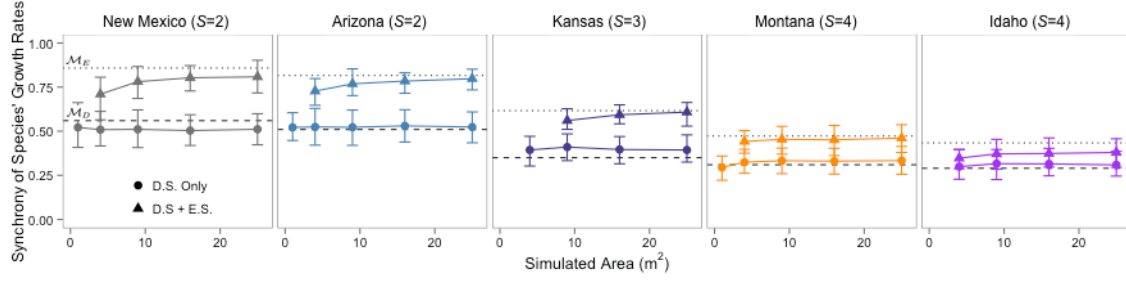
Figure 2: Synchrony of species' growth rates for each study area from IBM simulations across different landscape sizes when only demographic stochastcity is present ("D.S. Only") and when environmental stochasticity is also present removed ("D.S. + E.S."). The horizontal lines show the analytical predictions $\mathcal{M}_D$ (dashed line) and $\mathcal{M}_E$ (dotted line). The strength of demographic stochasticity decreases as landscape size increases because population sizes also increase. Theoretically, "D.S. Only" simulations should remain constant across landscape size, whereas "D.S. + E.S." simulations should shift from the $\mathcal{M}_D$ prediction to the $\mathcal{M}_E$ prediction as landscape size, and thus population size, increases, but only if demographic stochasticity it strong enough to counteract environmental forcing. Error bars represent the upper and lower 95% quantiles from model simulations.
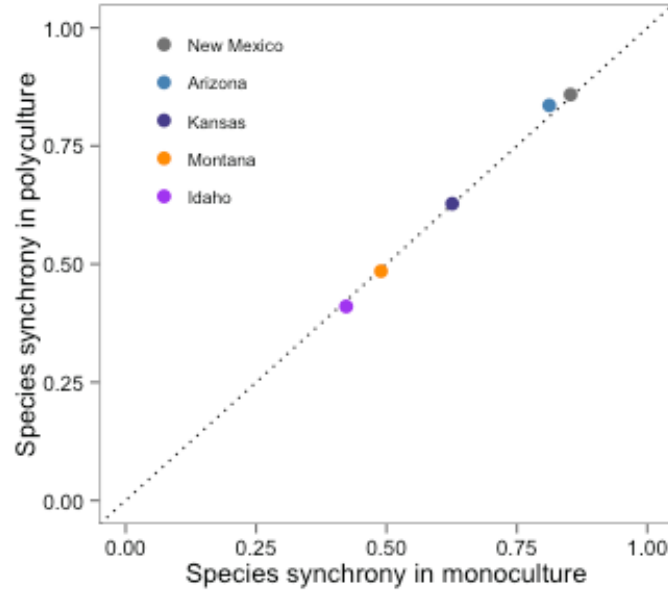
Figure 3: Synchrony of species per capita growth rates simulated in large monocultures (IPM without species interactions) versus synchrony in large polycultures (IPM with species interactions). We used the same sequence of random year effects for both simulations (monoculture and polyculture) to mimic biodiversity-ecosystem functioning experiments. The dashed line is the line of equality. Simulation results in this figure are analogous to "No Comp. + No D.S." (monocultures) and "No D.S." (polycultures) in Fig. 1, but here we control the time series of random year effects.